Work function of single-walled and multiwalled carbon nanotubes: First-principles study

W. S. Su,[1] T. C. Leung,[1,*] and C. T. Chan[2]
[1]*Department of Physics, National Chung Cheng University, Chia-Yi 621, Taiwan*
[2]*Department of Physics, Hong Kong University of Science and Technology, Clear Water Bay, Hong Kong, China*
and Institute of Nano Science and Technology, Hong Kong University of Science and Technology, Clear Water Bay, Hong Kong, China
(Received 30 April 2007; revised manuscript received 25 August 2007; published 11 December 2007)

Carbon nanotubes can be viewed as rolled-up graphene sheets. As such, their work functions should be closely related to those of graphene due to geometric and structural similarities. In this paper, we have systematically investigated the work functions of single-walled and multiwalled carbon nanotubes by density functional calculations. The work functions of single-walled carbon nanotubes (SWCNTs) are very close to those of graphene in the armchair conformation, while for the zigzag and chiral conformations, the work functions are close to those of graphene as the diameter is larger than a certain threshold. When the diameter of the tube is smaller than 10 Å, the work functions of zigzag and chiral tubes increase dramatically as the diameter decreases. The deviation in the work function from that of graphene for small tubes can be explained and qualitatively estimated by the downshift of the Fermi level due to the curvature effect. For multiwalled carbon nanotubes (MWCNTs), we only consider zigzag and armchair MWCNTs. We find that the work functions of all armchair and zigzag MWCNTs with inner tube diameters larger than 10 Å are very close to those of graphene. The work functions of zigzag MWCNTs with inner tube diameters smaller than 10 Å exhibit significant variations depending on the diameters of the inner and outer tubes. Using a very simple model, we find that the work functions of MWCNTs can be successfully estimated from the work functions and electronic structures of the constituent SWCNTs.

DOI: 10.1103/PhysRevB.76.235413 PACS number(s): 71.15.Mb, 73.30.+y, 73.20.−r, 73.22.−f

I. INTRODUCTION

Carbon nanotubes have attracted increasing attention from researchers since their discovery.[1] Because of their striking structural and electronic properties such as small diameters, high aspect ratios, high mechanical strength, and high thermal and chemical stability, carbon nanotubes are excellent field emitters and are thus potentially useful in field-emitting flat panel displays.[2] The work function of a carbon nanotube is a very important parameter in controlling the tube's field-emission properties. In addition, the work function is an important factor in controlling transport when the nanotube forms a junction. It is closely related to electronegativity and is thus important in the consideration of chemical reactivity.

Many studies have been conducted on the work functions of single-walled carbon nanotubes (SWCNTs). The estimation of the work function based on the Fowler-Nordheim model has, however, led to some uncertainties, such as if this simplified model is applicable to nanoemitters, particularly if the local geometry of the nanotubes is not measure. Ultraviolet photoemission spectroscopy (UPS) provides a model-independent measure of the work function. UPS experiments have estimated the work function to be 4.8 and 2.4 eV for SWCNT bundles and Cs-intercalated SWCNT bundles, respectively.[3] Using the transmission electron microscope technique, Gao *et al.*[4] measured the work function of individual multiwalled carbon nanotubes (MWCNTs) and reported the value of 4.6–4.8 eV. Moreover, using the photoelectron emission method, Shiraishi and Ata[5] measured the work functions of MWCNTs and SWCNTs and reported values of 4.95 and 5.05 eV, respectively. Meanwhile, Suzuki *et al.*[6] measured the work functions of 93 individual SWCNTs using photoemission electron microscopy and found that the work function of SWCNTs does not have a large structural dependence. Recent first-principles calculations show that the structure of the tips of SWCNTs will affect their work functions[7–9] and that the work functions of small tubes increase dramatically as the diameter of the tube decreases due to the curvature effect.[10] Using the charge equilibration model (CEM), Shan and Cho[11] proposed that the work functions of double-walled carbon nanotubes (DWCNTs) can be effectively approximated by the average of the inner and outer tubes. Up to now, however, there has been no systematic study on the work functions of MWCNTS. In this paper, we will therefore systematically study the work functions of SWCNTs and MWCNTs using density functional calculations. Initially, we examine the relationship between the work functions of SWCNTs and those of graphene. We also investigate the curvature effect on the work function of SWCNTs. Then, the results of MWCNTs, especially the work function of MWCNTs exhibiting significant variations depending on the diameters of the inner and outer tubes, are presented. Finally, we study the dependence of the work function of MWCNTs on its constituent SWCNTs using the simple charge transfer model, from which we can determine the work function of MWCNTs if we know the work function and the electronic structure of its constituent SWCNTs.

II. METHOD OF CALCULATIONS

The calculations are performed within the local density approximation (LDA) framework[12] using the Ceperley-Alder form of exchange-correlation functional and ultrasoft pseudopotentials[13] with a plane-wave cutoff of 358 eV. We used supercell geometries to calculate the work functions. In analyzing isolated SWCNTs and MWCNTs, the nanotubes

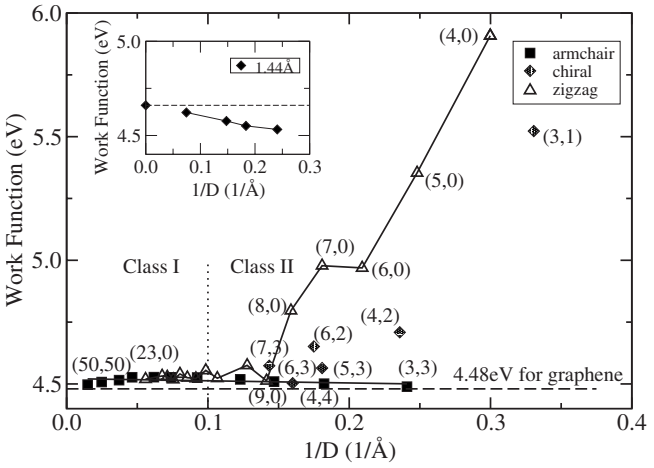

FIG. 1. Work functions of SWCNTs of different diameters (squares, armchair tubes; diamonds, chiral tubes; triangles, zigzag tubes). Lines serve as visual guides. The dashed line indicates the work function of graphene. The inset shows the work function of armchair (3,3), (4,4), (5,5), and (10,10) nanotubes calculated using the structure of Shan and Cho. The dashed line of the inset indicates the work function of graphene calculated using the structure of Shan and Cho.

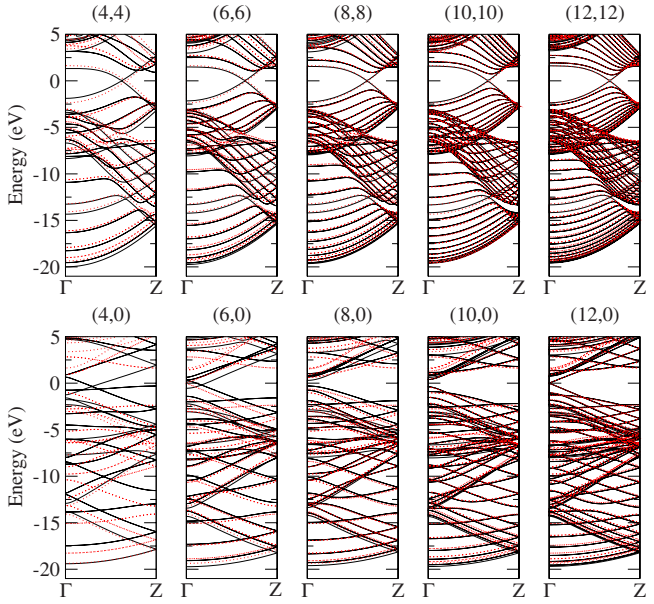

FIG. 2. (Color online) Band structures of SWCNTs of different diameters. Dashed line: results using a zone-folding approach. Solid line: LDA results.

are placed into a square array with intertube distances equal to 10 Å. At such a separation, the tube-tube interactions are very small so that the tubes can be treated as independent entities. For example, when we increase the intertube distance of the (3,3) tube from 10 to 20 Å, the calculated change of the work function is less than 0.003 eV. The length of the unit cell along the tube axis is determined by minimizing the total energy of the system. The k-point sampling was set to be $1\times1\times80$ for both SWCNTs and MWCNTs. All atoms were fully relaxed until the maximum magnitude of the force was less than 0.02 eV/Å. The work functions were determined from the difference between the Fermi level and the vacuum level. The Fermi energy is determined using the standard Gaussian smearing method with the width of the smearing in 0.1 eV. The vacuum level is defined as the average potential in the vacuum region where it approaches a constant. The Fermi level and the vacuum level must, of course, be determined from the same calculation for a meaningful result. In the case of semiconducting nanotubes, the Fermi level is chosen at the midgap.[10]

III. RESULTS AND DISCUSSION

We first considered the effect of the diameter and chirality on the work function of isolated SWCNTs with infinite lengths. We took into account the work functions of zigzag and armchair tubes, as well as the work function of a few chiral tubes such as (3,1), (4,2), (5,3), (6,2), (6,3), and (7,3) tubes. The work functions of isolated, infinite-length SWCNTs with diameters ranging from 2.8 to 67.3 Å are shown in Fig. 1. The work functions of armchair tubes fall within a narrow distribution, which is very close to the work function of graphene (~4.48 eV) and is independent of the diameter of the tube. We note that the work function of graphene is found to be 4.48 eV in our calculations, which is about 0.2 eV smaller than that obtained by Shan and Cho,[10] although the same formulation is used. This was due to the different lattice structures used in the calculations. In our calculations, the bond length was 1.41 Å, which was determined by minimizing the total energy of the graphene sheet, while the bond length in the study of Shan and Cho was 1.44 Å. They found that the work functions of armchair tubes decrease with a decrease diameter in small tubes, which is not the case in our results. This is due to the different atomic structures used in the calculations. Particularly, in our calculations, the length of the unit cell along the tube axis was obtained by minimizing the total energy of the system. In comparison, this length is fixed at the length given in the rolled-up graphene sheet with the bond length fixed at 1.44 Å in their study. To confirm that such differences originated from the atomic structure rather than from other details, we recalculated the work functions of the (3,3), (4,4), (5,5), and (10,10) armchair tubes using their atomic structure, and the results are shown in the inset of Fig. 1. The work functions of zigzag tubes with diameters greater than 10 Å are also close to those of graphene. However, the work functions of zigzag and chiral tubes with diameters smaller than 10 Å increase dramatically as the diameter decreases. The significant changes in the work functions of small tubes can be attributed to the curvature effect. It is interesting to note that the curvature effect on the work function of chiral tubes is smaller than that on zigzag tubes.

Figure 2 compares the band structure of various armchair and zigzag tubes calculated by LDA (solid line) with that obtained from the zone folding (dashed line) calculation of graphene by LDA dispersion. In the zone-folding approach, it is well known and well understood that the Fermi wave vector (pinned at the crossing point of two bands) for all armchair tubes is located exactly at $k_F=2\pi/3T$, where T is

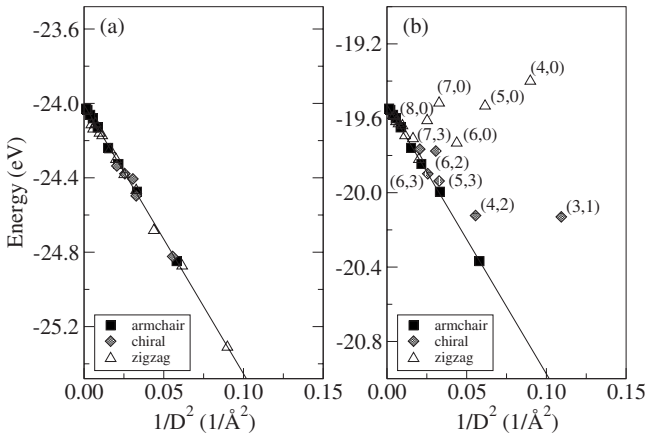

FIG. 3. (a) The lowest eigenvalues relative to the vacuum level at the Γ point of SWCNTs of different diameters (squares, armchair SWCNTs; diamonds, chiral SWCNTs; triangles, zigzag SWCNTs). The solid line is a linear fit to the data of various SWCNTs. (b) Same plot as (a) but shown with eigenvalues relative to the Fermi level. The solid line is a linear fit to the data of armchair SWCNTs.

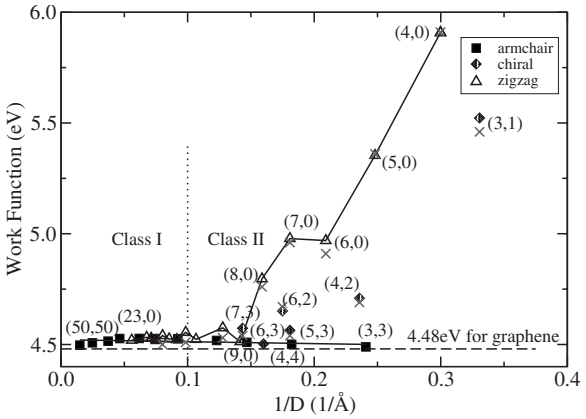

FIG. 4. Work functions of SWCNTs of different diameters [squares, armchair tubes; diamonds, chiral tubes; triangles, zigzag tubes; crosses, calculated by Eq. (1)]. Lines serve as visual guides.

the translation lattice constant of the tube. However, for the real armchair tube structure, when the curvature effect is properly taken into account, the position of the Fermi wave vector is slightly shifted toward the zone center, and the amount of k_F downshift is proportional to $1/D^2$.[14] Nevertheless, the change in Fermi energy relative to the vacuum is negligible; the work function of all armchair tubes is therefore very close to that of graphene. On the other hand, the curvature effect downshifts the binding state of the *s*-like σ band, and then the position of the lowest eigenvalue at the Γ point shifts down as shown in the upper panel of Fig. 2. In small zigzag tubes, the σ orbital mixing into the π states, which is caused by the curvature effect of the tube, decreases the energy of the singly degenerate π^* states,[15,16] as shown in the lower panel of Fig. 2. This will downshift the Fermi energy relative to the vacuum level and thus increase the work function.

In order to estimate the amount of the downshift of the Fermi energy relative to the vacuum level due to the curvature effect, we studied the band structure of SWCNTs, and in Fig. 3(a), we show the lowest eigenvalue ($\tilde{\varepsilon}_b^\Gamma$) of the valence bands relative to the vacuum level at the Γ point for various SWCNTs. Our study's results show that it can be fitted by a straight line given by $\tilde{\varepsilon}=-24.01-14.46/D^2$, where D is the diameter of the tube. On the other hand, in Fig. 3(b), we plot the lowest eigenvalue (ε_b^Γ) of the valence bands relative to the Fermi energy at the Γ point for various SWCNTs. The lowest eigenvalues of the valence bands of all the armchair tubes are also linear as given by $\varepsilon=-19.53-14.48/D^2$. An extrapolation toward a larger radius limit gives a value of −19.53 eV, which is the lowest eigenvalue of the valence band of graphene at the Γ point. The lowest eigenvalues for small zigzag and chiral tubes are off the line. The *s*-*p* mixing in the small zigzag and chiral radius tubes lowers the energies of some unoccupied states to below the Fermi level of graphene. This leads to a higher density of states below the Fermi level of graphene, so that when electrons are being filled up from the bottom of the valence band, the zigzag tubes "fill up earlier" than the armchair tubes. This then leads to a lower energy of the Fermi energy relative to the vacuum or, equivalently, a higher work function measure. The amount of deviation in the lowest eigenvalue at the Γ point from the line is equal to the change of its Fermi energy relative to the vacuum level caused by the curvature effect. Therefore, the work function of the tube can be given by the sum of the work function of graphene and the deviation of its lowest eigenvalue relative to the Fermi energy at the Γ point away from the line as follows:

$$\Phi_{SWCNT}=\Phi_{graphene}+\varepsilon_b^\Gamma-(-19.53-14.48/D^2). \quad (1)$$

Figure 4 shows the work functions calculated by Eq. (1) and by real LDA calculations. The overall agreement indicates that the deviation of the work function of SWCNTS from that of graphene is dominated by the curvature effect. This means that we can calculate the work function of any SWCNT using only its band structure information and without knowing the vacuum level.

In the following section, we consider the work functions of multiwalled carbon nanotubes and show that the work functions of multiwalled tubes can be predicted from those of MWCNTs constituent single-walled tubes. The double-walled carbon nanotube (DWCNT) is the simplest type of the MWCNT, and its intertube distance is known to be 3.24–3.44 Å from experimental measurements,[17] which is close to the interlayer separation of graphite. In principle, a MWCNT can be composed of a pair of inner and outer constituent layers with any chirality. Constrained by the requirement of a reasonably small unit cell for the LDA calculations, we only consider MWCNTs made up of concentric rings of tubes of the same chirality (i.e., armchair@armchair@armchair$\cdots$ or zigzag@zigzag@zigzag$\cdots$). In our calculations for MWCNTs, we use $(n,0)@(n+9,0)@(n+18,0)@(n+27,0)\cdots$ for zigzag MWCNTs and $(n,n)@(n+5,n+5)@(n+10,n+10)@(n+15,n+15)\cdots$ for armchair MWCNTs. The intertube distance is 3.35–3.39 Å for armchair MWCNTs and is 3.41–3.52 Å for zigzag MWCNTs. We first focus on double-walled nanotubes. The work func-

TABLE I. Work function (Φ) and intertube distance (Δd_{12}) for various armchair and zigzag DWCNTs calculated by LDA.

	Armchair					
	(4,4)@(9,9)	(5,5)@(10,10)	(6,6)@(11,11)	(7,7)@(12,12)	(8,8)@(13,13)	(9,9)@(14,14)
Φ (eV)	4.53	4.53	4.54	4.53	4.53	4.53
Δd_{12} (Å)	3.35	3.35	3.37	3.38	3.38	3.38
	Zigzag					
	(4,0)@(13,0)	(5,0)@(14,0)	(6,0)@(15,0)	(7,0)@(16,0)	(8,0)@(17,0)	(9,0)@(18,0)
Φ (eV)	4.99	4.91	4.64	4.84	4.72	4.53
Δd_{12} (Å)	3.41	3.44	3.45	3.46	3.47	3.47

tions for various armchair and zigzag tubes calculated by LDA are given in Table I. Since the work function of isolated armchair SWCNTs is close to that of graphene, the work function of isolated armchair DWCNTs should also be close to that of graphene. This is indeed borne out by the LDA results. In isolated zigzag DWCNTs, the work function is expected to be nearly the same as that of graphene when its inner tube is larger than 10 Å. This is also verified in the LDA calculations. If the inner tubes have diameters smaller than 10 Å and if the tubes are not armchair tubes, then the work functions of the constituent SWCNTs in the MWCNT are different, and we expect some changes. The results in Table I show that the work functions for zigzag tubes exhibit significant variations depending on the diameters of the inner tube and outer tubes.

We calculated the redistribution of charge density due to the charge transfer from the outer tube to the inner tube, which is defined as

$$\Delta\rho(\vec{r}) = \rho(\vec{r}) - [\rho_{in}(\vec{r}) + \rho_{out}(\vec{r})], \tag{2}$$

where $\rho(\vec{r})$ is the charge density of the DWCNT, and ρ_{out} (ρ_{in}) is the charge density of the isolated outer (inner) tube, which is generated by removing the inner (outer) tube with all the outer (inner) tube's atoms frozen at the original position. Figures 5(a) and 5(b) show the contour plot of the redistributed charge density for (4,0)@(13,0) and (5,0)@(14,0), respectively. It is visually obvious that the charge is transferred from the outer tube to the inner tube in both cases. In order to better understand these observations,

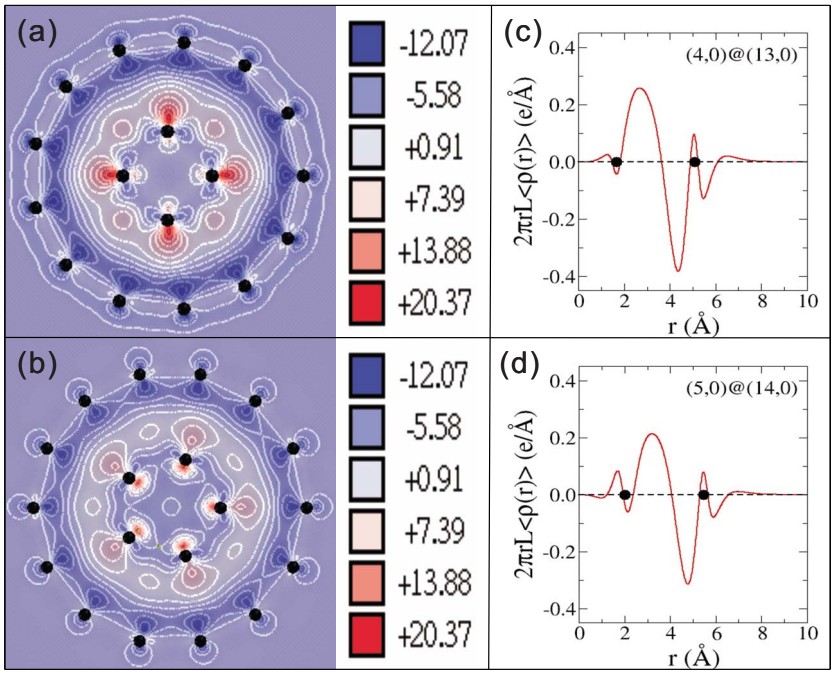

FIG. 5. (Color online) Contour plots of the redistributed charge density of (a) (4,0)@(13,0) DWCNTs and (b) (5,0)@(14,0) DWCNTs. Plots are on the plane perpendicular to the tube axis, with black circles denoting the position of carbon atoms. The calculated averages of the redistributed charge density in (4,0)@(13,0) and (5,0)@(14,0) are also shown in (c) and (d), respectively.

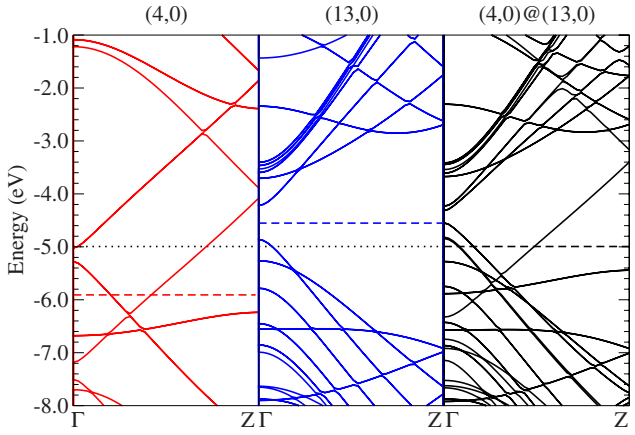

FIG. 6. (Color online) The band structures calculated by LDA for an individual (4,0) nanotube, an individual (13,0) nanotube, and (4,0)@(13,0) DWCNTs. The vacuum level is set to zero. The work functions of the (4,0), (13,0), and (4,0)@(13,0) tubes are 5.93, 4.54, and 4.99 eV, respectively. The dashed line is the Fermi level of the system. The dotted lines serve as visual guides.

we calculated the average of the redistributed charge density given by

$$\langle \Delta\rho(\vec{r})\rangle = \frac{1}{2\pi L}\int_0^{2\pi} d\theta \int_0^L \Delta\rho(\vec{r})dz. \tag{3}$$

The averages of the redistributed charge density in (4,0)@(13,0) and (5,0)@(14,0) are shown in Figs. 5(c) and 5(d), respectively. We can see that in both cases, there is a depletion of electronic charge from the outer tube and an increase in electronic charge in the inner tube.

To understand the work function variations, we first consider the case of a (4,0)@(13,0) DWCNT. In such a case, the inner tube has an ultrasmall radius which has strong curvature effects on its own work function, thereby affecting the work function of the double-walled tube as a composite system. We note that if the inner tube has a very small radius, it is generally a metal. If the inner tube has a larger radius, it can be a semiconductor, which we will discuss in the next section. Here, we focus on metal tubes. We show the calculated band structures by LDA for an individual (4,0) nanotube, an individual (13,0) nanotube, and (4,0)@(13,0) DWCNTs in Fig. 6, where the vacuum level (set at 0 eV) is aligned so that the different electron affinities of the tubes are apparent. After aligning the vacuum levels, we can see that the highest occupied (HO) state of the outer tube is higher in energy than that of the inner tube. Therefore, we expect a transfer of electrons from the outer tube to the inner tube until the potentials of the inner and outer tubes become equal as shown in explicit charge calculations in Fig. 5. We can simplify the notion of charge transfer by considering a dipole cylindrical sheet formed between the inner and the outer tubes, leading to a potential barrier ΔV as shown schematically in Fig. 7. The Fermi level will be pinned at an energy ΔE_{out}, which is below the energy of the HO state of the outer tube, where ΔE_{out} is the downshift of the Fermi level of the

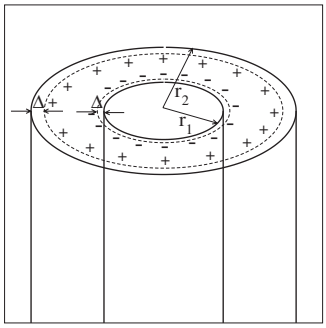

FIG. 7. A schematic diagram of a cylindrical capacitor for the charge transfer model of DWCNTs. The effective radius is $r_1+\Delta$ and $r_2-\Delta$ for the inner and outer tubes, respectively, where r_1 and r_2 are the radius of inner and outer tubes and Δ is equal to 1.0 Å.

outer tube due to the charge transfer. Therefore, the HO states of the outer and inner tubes after the charge transfer can be computed as

$$\tilde{\varepsilon}_{out}^{HO} = \varepsilon_{out}^{HO} - \Delta E_{out}, \tag{4}$$

$$\tilde{\varepsilon}_{in}^{HO} = \varepsilon_{in}^{HO} + \Delta E_{in} + \Delta V, \tag{5}$$

where ε_{out}^{HO} and ε_{in}^{HO} are the highest occupied states of the outer and inner tubes before the charge transfer, respectively, and ΔV is the potential barrier between the inner and outer tubes. Using the simplest possible model, ΔV is given by $\frac{q}{2\pi\varepsilon_0 L}\ln\frac{r_{out}-\Delta}{r_{in}+\Delta}$, where q is the amount of the charge transfer, r_{out} (r_{in}) is the radius of the outer (inner) tube, and Δ is set to be 1.0 Å, which is suggested by inspecting Fig. 5. We will show later that the work function estimated by our model is only weakly dependent on the value of Δ, which is nonzero since the excess charges due to the charge transfer are slightly displaced with respect to the atomic positions. By equating $\tilde{\varepsilon}_{out}^{HO}$ and $\tilde{\varepsilon}_{in}^{HO}$, we generate the following equations which can be used to determine ΔE_{out} by the band structure of the inner and outer tubes:

$$\varepsilon_{in}^{HO} + \Delta E_{in} + \frac{q}{2\pi\varepsilon_0 L}\ln\frac{r_{out}-\Delta}{r_{in}+\Delta} = \varepsilon_{out}^{HO} - \Delta E_{out}, \tag{6}$$

$$q = \int_{\varepsilon_{in}^{HO}}^{\varepsilon_{in}^{HO}+\Delta E_{in}} D_{in}(\varepsilon)d\varepsilon = \int_{\varepsilon_{out}^{HO}-\Delta E_{out}}^{\varepsilon_{out}^{HO}} D_{out}(\varepsilon)d\varepsilon, \tag{7}$$

where L is the length of the tube within the unit cell, $D_{out}(\varepsilon)$ ($D_{in}(\varepsilon)$) are the densities of states of the outer (inner) tube, and ΔE_{out} can be given by solving Eqs. (6) and (7), requiring the self-consistency of the value of q. The isolated tube densities of states are used to calculate the charge transfer in Eqs. (6) and (7). For a given trial value of ΔE_{out}, we can evaluate the values of q and ΔE_{in} using Eq. (7). We then check whether Eq. (6) is satisfied. If not, we increase the value of ΔE_{out} by a small amount $\Delta\varepsilon$ and iterate the process until Eq. (6) can be satisfied. The condition of self-consistency depends on the choice of $\Delta\varepsilon$, and it can be as small as we want. In the calculation, the value of $\Delta\varepsilon$ is 0.01 eV. The amounts of charge transfer from the outer tube

TABLE II. Work functions for various MWCNTs calculated by LDA, model of Shan and Cho, and our model.

	Work function (eV)				
			Our model		
	VASP (LDA)	CEM	$\Delta=0.9$ Å	$\Delta=1.0$ Å	$\Delta=1.1$ Å
(4,0)@(13,0)	4.99	5.23	4.98	4.99	5.02
(5,0)@(14,0)	4.91	4.94	4.90	4.91	4.91
(6,0)@(15,0)	4.64	4.72	4.62	4.62	4.63
(7,0)@(16,0)	4.84	4.76	4.81	4.81	4.81
(8,0)@(17,0)	4.72	4.66	4.65	4.65	4.65
(9,0)@(18,0)	4.53	4.52	4.52	4.52	4.52
(10,0)@(19,0)	4.56	4.55	4.53	4.53	4.53
(11,0)@(20,0)	4.53	4.51	4.52	4.52	4.52
(12,0)@(21,0)	4.54	4.52	4.53	4.53	4.53
(13,0)@(22,0)	4.55	4.54	4.53	4.53	4.53
(14,0)@(23,0)	4.54	4.52	4.52	4.52	4.52
(15,0)@(24,0)	4.54	4.53	4.53	4.53	4.53
(22,0)@(31,0)	4.53	4.52	4.52	4.52	4.52
(4,0)@(13,0)@(22,0)	4.77	4.88	4.76	4.78	4.79
(5,0)@(14,0)@(23,0)	4.76	4.73	4.75	4.76	4.76
(6,0)@(15,0)@(24,0)	4.57	4.62	4.56	4.56	4.57
(7,0)@(16,0)@(25,0)	4.74	4.64	4.72	4.72	4.73
(8,0)@(17,0)@(26,0)	4.66	4.59	4.57	4.57	4.57
(4,0)@(13,0)@(22,0)@(31,0)	4.66	4.70	4.69	4.69	4.70
(5,0)@(14,0)@(23,0)@(32,0)	4.67	4.62	4.68	4.69	4.69
(6,0)@(15,0)@(24,0)@(33,0)	4.54	4.57	4.53	4.54	4.54
(7,0)@(16,0)@(25,0)@(34,0)	4.63	4.58	4.67	4.67	4.67
(8,0)@(17,0)@(26,0)@(35,0)	4.62	4.55	4.51	4.51	4.51

to the inner tube calculated by the above process are 0.26, 0.17, and 0.09 electrons per period for (4,0)@(13,0), (5,0)@(14,0), and (6,0)@(15,0), respectively. The value of the work function is equal to the absolute value of the energy of its outer tube's HO state, which is given by Eq. (4), due to the selection of the vacuum level energy as a zero point.

The work of Shan and Cho showed that the work function of the DWCNT can be approximated effectively by the average of the work functions of the inner and outer tubes. This amounts to neglecting the potential barrier ΔV between the inner and outer tubes due to the charge transfer and the setting of the hardness of the tubes to a constant, which effectively uses a constant to approximate the density of states of the tubes. In our calculations, as shown in Fig. 6 for the case of (4,0)@(13,0), the density of states below the Fermi level of the (13,0) tube is larger than that above the Fermi level of the (4,0) tube. We found that ΔE_{out} is about equal to 0.15 eV and ΔE_{in} is about 0.3 eV. The potential barrier is about 0.6 eV, which is not that small. Table II shows the work functions for a few MWCNTs calculated by real LDA calculation, our model, and the method of Shan and Cho. The extension to triple-walled carbon tubes will be discussed in the following sections. We can see that our study's results have a better agreement compared with those of the other methods. We particularly note that our LDA results are different from the LDA results of Shan and Cho for some DWCNTs. This is due to the difference in the structure involved in the calculations. In our calculations, the length of the unit cell along the tube axis is obtained by minimizing the total energy of the system.

If the outer and inner tubes are both semiconductor tubes, we find that there is a negligible charge transfer when the highest occupied state of the outer tube is lower than the lowest unoccupied (LU) state of the inner tube as in the case of the (8,0)@(17,0) tube. Figure 8 shows the LDA calculated band structures for an individual (8,0) nanotube, an individual (17,0) nanotube, and (8,0)@(17,0) DWCNTs. We again set the vacuum level to 0 eV. In this case, the work function of the DWCNT is simply

$$\Phi = \frac{1}{2}\mathrm{abs}\{\varepsilon_{out}^{HO} + \min[\varepsilon_{out}^{LU}, \varepsilon_{in}^{LU}]\}, \tag{8}$$

where ε_{out}^{LU} (ε_{in}^{LU}) is the lowest unoccupied state of the outer (inner) tube. It is worth noting that the HO and LU bands of the inner tube shift down by about 0.1 eV relative to the outer tube in our real LDA calculation for the (8,0)@(17,0) tube. This explains the observation that the work function is

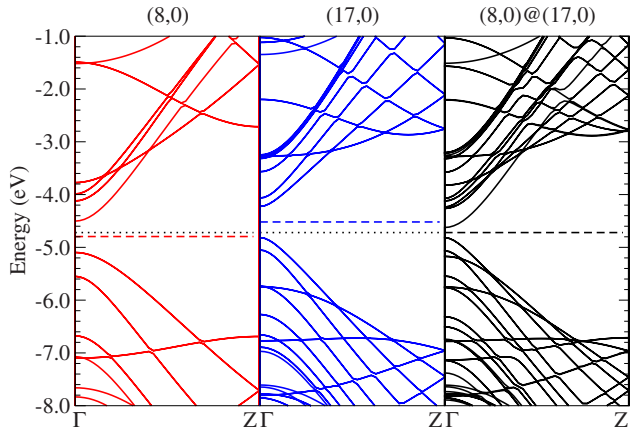

FIG. 8. (Color online) The band structures calculated by LDA for an individual (8,0) nanotube, an individual (17,0) nanotube, and (8,0)@(17,0) DWCNTs. The vacuum level is set to zero. The work functions of the (8,0), (17,0), and (8,0)@(17,0) tubes are 4.80, 4.52, and 4.72 eV, respectively. The dashed line is the Fermi level of the system. The dotted lines serve as visual guides.

underestimated by about 0.05 eV in our model of the (8,0)@(17,0) tube.

Using the above process, we can thus obtain the work function of any DWCNT from the work function and the band structure of its constituent SWCNTs. The band structure of the DWCNT can also be calculated after we find ΔE_{in} and ΔE_{out} during the above process. The DWCNT band structure is the superposition of the band structures of its constituent SWCNTs with appropriate shifts. The Fermi level is now pinned at ΔE_{out} below its highest occupied state for its outer tube and at ΔE_{in} above its highest occupied state for its inner tube. Figure 9 shows the band structure of the (4,0)@(13,0) tube calculated by LDA and our superposition model. The agreement is good. Therefore, as long as we have the work function and band structure of all constituent SWCNTs, we can calculate the work function and band structure of any DWCNT by employing the above-mentioned process. We note that we do not need to do the LDA calculation for large SWCNTs. We can simply use the band structure calculated from the zone folding of LDA dispersion of graphene and the work function of graphene for large SWCNTs.

The process employed above can be iterated from the interior to the exterior to find the work function and band structure of any triple-walled carbon nanotube. Now, Eqs. (6) and (7) can be rewritten as

$$\varepsilon_I^{HO} + \Delta E_I + \frac{q}{2\pi\varepsilon_0 L} \ln \frac{r_{out} - \Delta}{r_I + \Delta} = \varepsilon_{out}^{HO} - \Delta E_{out}, \tag{9}$$

$$q = \int_{\varepsilon_I^{HO}}^{\varepsilon_I^{HO}+\Delta E_I} D_I(\varepsilon)d\varepsilon = \int_{\varepsilon_{out}^{HO}-\Delta E_{out}}^{\varepsilon_{out}^{HO}} D_{out}(\varepsilon)d\varepsilon, \tag{10}$$

where q is the amount of the charge transfer from the inner double-walled tube to the outermost tube, ε_{out}^{HO} (ε_I^{HO}) is the highest occupied state in energy before the charge transfer,

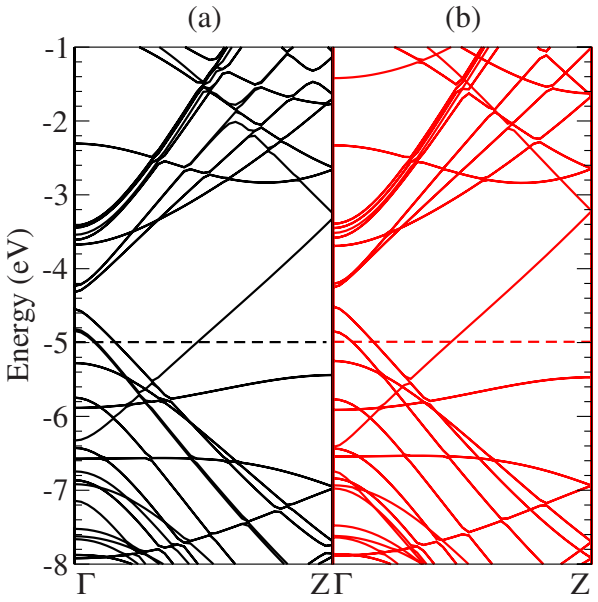

FIG. 9. (Color online) The band structures of a (4,0)@(13,0) tube calculated by (a) LDA and (b) charge transfer model. The dashed line is the Fermi level of the system.

$D_{out}(\varepsilon)$ [$D_I(\varepsilon)$] is the density of states, and r_{out} (r_I) is the radius of the outer (inner double-walled) tube. The ΔE_{out} can be determined by solving Eqs. (9) and (10) requiring the self-consistency of the value of q. The value of the work function is equal to the absolute value of the energy of its outer tube's HO state. When the outer and inner tubes are both semiconductor tubes, Eq. (8) can be rewritten as

$$\Phi = \frac{1}{2}\text{abs}\{\varepsilon_{out}^{HO} + \min[\varepsilon_{out}^{LU}, \varepsilon_I^{LU}]\}, \tag{11}$$

where ε_{out}^{LU} (ε_I^{LU}) is the lowest unoccupied state of the outer (inner double-walled) tube.

It is then obvious that we can generalize the Eqs. (9)–(11) to calculate the work functions and band structures of any N-walled nanotubes. We set q to be the amount of the charge transfer from the outer nanotube to the inner $(N-1)$-walled nanotube, ε_{out}^{HO} (ε_I^{HO}) is the highest occupied state in energy before the charge transfer, $D_{out}(\varepsilon)$ [$D_I(\varepsilon)$] is the density of states, r_{out} (r_I) is the radius, and ε_{out}^{LU} (ε_I^{LU}) is the lowest unoccupied state of the outer [inner $(N-1)$-walled] nanotube. In Table II, we show the work functions of various MWCNTs calculated by fully fledged LDA calculation, the CEM model, and the charge transfer model for different values of Δ. The results calculated by the charge transfer model are generally better than that calculated by the CEM model. We see that the result in the charge transfer model is not sensitive to the choice of the value of Δ. Figure 10 shows the work functions of various zigzag N-walled nanotubes calculated by LDA calculations and the charge transfer model. We note that metallicity plays an important rule in the work function of MWCNTs. For instance, the MWCNTs with inner tube (6,0) shows a characteristic low work function. This can be explained by our model. As pointed out before, the

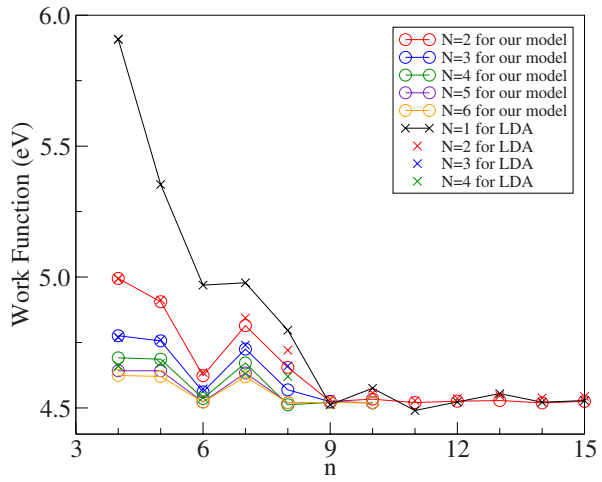

FIG. 10. (Color online) Work functions of various zigzag N-walled nanotubes with $(n,0)$ inner tube, calculated by the charge transfer model (circles) for $\Delta=1.0$ Å and real LDA calculation (crosses). Lines serve as visual guides.

work functions of SWCNT with a diameter larger than 10 Å are close to those of graphene. Therefore, the work function of the outer tube for any DWCNT with an inner tube greater than (4,0) is close to 4.5 eV. In our method, the work function of the DWCNT is given by the absolute value of the energy of its outer isolated tube's HO state plus the value of the downshift of the Fermi level due to the charge transfer. When the outer tube is metallic, the highest occupied state is the same as the Fermi level. The work function of SWCNT is equal to the absolute value of its Fermi level due to the selection of the vacuum level as zero. The work function of the DWCNT is given by 4.5 eV$+\Delta E_{out}$, where ΔE_{out} is the downshift of the Fermi level due to the charge transfer. For the case in which its outer tube is a semiconductor, the highest occupied state is equal to the Fermi level plus one half of the value of its band gap. Therefore, the work function is given by 4.5 eV$+\Delta E_{out}+E_g/2$. This explains why the metallic MWCNT shows a characteristic low work function.

It is interesting to note that the work functions of the MWCNTs exhibit noticeable variations depending on the diameters of the inner and outer tubes. The agreement between our method with real LDA calculations indicates that our model can provide an efficient and accurate method to estimate to work functions of MWCNTs. This is in contrast to the difficulty involved in calculating using brute force, that is, using the work function and band structure of SWCNTs, which can be readily done.

IV. CONCLUSIONS

In conclusion, we have systematically investigated the work functions of SWCNTs and MWCNTs by density functional calculations. The work functions of armchair tubes of any diameter and large tubes with any chirality are very close to those of graphene. The work functions of zigzag and chiral tubes with diameters smaller than 10 Å increase dramatically as the diameter of the tube decreases. The significant changes in the work function of small tubes is due to the curvature effect, which decreases the energy of the singly degenerate π^* states and downshifts the Fermi level relative to the vacuum level, thereby increasing the work function. Using an intuitive charge transfer model, we can calculate the work function of any MWCNT from the work function and the electronic band structure of its constituent SWCNTs. We find that the work functions of MWCNTs exhibit noticeable variations depending on the diameters of the inner and outer tubes.

ACKNOWLEDGMENTS

We acknowledge the National Center for Theoretical Sciences (NCTS) in Taiwan and financial support from the National Science Council (NSC) of Taiwan under Grants No. NSC-95-2112-M194-015 and No. NSC-95-2120-M002-014, from the Research Grant Council of Hong Kong through Central Allocation Grant No. CA04/05.SC02, and from a grant of computer time at the National Center for High Performance Computing in Taiwan.

*Corresponding author; tcleung@phy.ccu.edu.tw

[1] S. Iijima, Nature (London) **354**, 56 (1991).
[2] Q. H. Wang, A. A. Setlur, J. M. Lauerhaas, J. Y. Dai, E. W. Seelig, and R. P. H. Chang, Appl. Phys. Lett. **72**, 2912 (1998).
[3] S. Suzuki, C. Bower, Y. Watanabe, and O. Zhou, Appl. Phys. Lett. **76**, 4007 (2000).
[4] R. Gao, Z. Pan, and Z. L. Wang, Appl. Phys. Lett. **78**, 1757 (2001).
[5] M. Shiraishi and M. Ata, Carbon **39**, 1913 (2001).
[6] S. Suzuki, Y. Watanabe, Y. Homma, S. Y. Fukuba, S. Heun, and A. Locatelli, Appl. Phys. Lett. **85**, 127 (2004).
[7] C. W. Chen and M. H. Lee, Nanotechnology **15**, 480 (2004).
[8] J. Zhao, J. Han, and J. P. Lu, Phys. Rev. B **65**, 193401 (2002).
[9] W. S. Su, T. C. Leung, Bin Li, and C. T. Chan, Appl. Phys. Lett. **90**, 163103 (2007).
[10] B. Shan and K. Cho, Phys. Rev. Lett. **94**, 236602 (2005).
[11] B. Shan and K. Cho, Phys. Rev. B **73**, 081401(R) (2006).
[12] G. Kresse and J. Hafner, Phys. Rev. B **47**, 558 (1993); **49**, 14251 (1994); G. Kresse and J. Furthmuller, Comput. Mater. Sci. **6**, 15 (1996).
[13] G. Kresse and J. Hafner, J. Phys.: Condens. Matter **6**, 8245 (1994).
[14] V. Zolyomi and J. Kurti, Phys. Rev. B **70**, 085403 (2004).
[15] X. Blasé, Lorin X. Benedict, Eria L. Shirley, and Steven G. Louie, Phys. Rev. Lett. **72**, 1878 (1994).
[16] S. Reich, C. Thomsen, and P. Ordejon, Phys. Rev. B **65**, 155411 (2002).
[17] J. Wei, B. Jiang, X. Zhang, H. Zhu, and D. Wu, Chem. Phys. Lett. **376**, 753 (2003).